

Optical detection of electron paramagnetic resonance in electron-irradiated GaN

C. Bozdog, H. Przybylinska,* and G. D. Watkins
Department of Physics, Lehigh University, Bethlehem, Pennsylvania 18015

V. Härle and F. Scholz
4. Physikalisches Institut, Universität Stuttgart, D-70550 Stuttgart, Germany

M. Mayer and M. Kamp
Abteilung Optoelektronik, Universität Ulm, D-89081 Ulm, Germany

R. J. Molnar
Massachusetts Institute of Technology/Lincoln Laboratory, 244 Wood Street, Lexington, Massachusetts 02173

A. E. Wickenden, D. D. Koleske, and R. L. Henry
Naval Research Laboratory, Code 6861, Washington, D.C. 20375-5347
 (Received 17 December 1998)

2.5 MeV electron irradiation of wurtzite GaN epitaxially grown on sapphire substrates greatly reduces its near-UV and visible luminescence, producing two bands in the near infrared. In one of these, a broad structureless band centered at ~ 0.95 eV, three optically detected $S=1/2$ electron paramagnetic resonances (ODEPR) are observed. Two of these display well-resolved hyperfine interaction with a single Ga nucleus, suggesting that they are interstitial-Ga related. The second band has a sharp zero-phonon line at 0.88 eV and accompanying phonon-assisted structure and reveals an $S=1$ ODEPR signal, as yet not identified.
 [S0163-1829(99)05719-7]

There is considerable current interest in the role of point defects in GaN, stimulated by the successful application of it and its alloys in blue light emitting and laser diode devices, and their potential for high-temperature electronic device application.¹ The main focus of the present investigation is the characterization of the intrinsic defects—vacancies and interstitials on the two sublattices. Since essentially nothing is known concerning these important defects in GaN, this study represents an attempt to unravel their properties using magnetic resonance techniques.

Our approach is to study by optical detection of electron paramagnetic resonance (ODEPR) the effect of 2.5 MeV electron irradiation on the photoluminescence properties of the material. The primary defects produced in such an irradiation are vacancies and interstitials on each sublattice. We therefore can expect the defects produced by the irradiation to be related to these intrinsic defects, either singly isolated, or, if mobile, as trapped by other defects. In two previous brief reports,^{2,3} we have described preliminary ODEPR results on a single irradiated thin-film sample grown on sapphire. The present paper provides the first detailed description of these results, including analysis and discussion of the spectra observed. In addition, the work has been greatly expanded, including the study of several additional samples from separate sources, and the observation of an important additional ODEPR spectrum.

I. EXPERIMENTAL PROCEDURE

The samples investigated were all films of wurtzite GaN grown on sapphire. Their origin, method of growth, and other properties are given in Table I. After a brief photo-

luminescence (PL) and optical detection of electron-paramagnetic-resonance (PLODEPR) characterization in the as-grown state, the samples were irradiated at room temperature with electrons from a 2.5 MeV van de Graaff accelerator. Although the effect of irradiation could already be seen after 5×10^{17} e/cm², the typical dosage was $\sim 1.5 \times 10^{18}$ e/cm². Isochronal anneals of two of the samples (one each from groups A and B) were subsequently performed. These were performed in closed quartz ampoules under N₂ gas at pressure slightly above one atmosphere.

The PL and PLODEPR were performed under excitation with the various ultraviolet (UV), visible, or near-infrared (IR) lines available from either a He-Cd (3.82 eV), Ar⁺ ion (3.53, 3.41, 2.73–2.41 eV), or tunable Ti-sapphire laser (1.61–1.52 eV). The typical excitation power was ~ 20 mW. Detection of the luminescence was achieved in the visible and near-UV by a silicon diode (EGG 250 UV) and in the near-IR by a cooled Ge detector (North Coast EO817S), followed by lockin detection synchronized to the frequency of a chopper in the excitation (for PL), or to the microwave on-off modulation frequency (for PLODEPR). All PL and PLODEPR studies were performed at pumped liquid He (~ 1.7 K) in a 35 GHz ODEPR spectrometer which has been described elsewhere.⁴ For the spectral dependence of the PL or PLODEPR, a 1/4 m Jarrell-Ash monochromator was inserted before detector.

II. EXPERIMENTAL RESULTS

A. As grown

Figure 1 summarizes the visible PL and associated PLODEPR signals before irradiation. In samples A, B, and

TABLE I. GaN samples studied. All were grown on sapphire substrates.

Samples	Source	Growth method	Thickness (μm)	Carrier type, conc. (cm^{-3})	Nucleation (buffer) layer
A	Stuttgart U.	MOVPE ^a	1, 3	<i>n</i> -, mid- 10^{16}	125, 1000 Å, AlN
B	NRL	MOVPE ^b	2.4	semi-ins.	~ 200 Å, AlN
C	MIT/Lincoln	HVPE ^c	61.3	<i>n</i> -, mid- 10^{16}	ZnO pre-treatment
D	Ulm U.	MBE ^d	1.8, 11.0	<i>n</i> -, $2-3 \times 10^{17}$	GaN

^aF. Scholz, V. Härle, H. Bolay, F. Steuber, B. Kaufmann, G. Reyher, A. Dörnen, O. Gröfer, S.-J. Im, and A. Hangleiter, *Solid State Electron.* **41**, 141 (1997).

^bA. E. Wickenden, D. K. Gaskill, D. D. Koleske, K. Doverspike, D. S. Simons, and P. H. Chi, in *Gallium Nitride and Related Materials*, edited by F. A. Ponce, R. D. Dupuis, S. Nakamura, and J. A. Edmond, MRS Symposia Proceedings No. 395 (Materials Research Society, Pittsburgh, 1996), p. 679.

^cR. J. Molnar, W. Goetz, L. T. Romano, and N. M. Johnson, *J. Cryst. Growth* **178**, 147 (1997).

^dM. Kamp, M. Mayer, A. Pelzmann, and K. J. Eberling, *MRS Internet J. Nitride Semicond. Res.* **2**, 26 (1997).

D, the dominant luminescence is the much studied 2.2 eV “yellow” band as shown in Fig. 1(a), and the two ODEPR signals detected in it are the usual ones observed,^{5–7} the shallow effective-mass donor (EM) and deeper DD defect, as illustrated in Fig. 1(b). The visible luminescence in the hydride vapor phase epitaxy (HVPE) sample C, however, contains an additional and stronger red band at ~ 1.8 eV,⁸ as shown in Fig 1(c). The ODEPR for it also differs, as shown in Fig. 1(d) in that a different deep defect signal that we label L1 dominates along with the EM signal. The spectral dependence of the EM signal shown in Fig. 1(e) reveals that it is involved in both the 2.2 eV and stronger 1.8 eV PL, but that of L1, shown in Fig. 1(f), reveals that it is associated only with the “red” 1.8 eV band. Like the yellow band therefore the red band also results from a spin dependent electron

transfer from the shallow donor to a deep, but different defect, as characterized by L1. We will find that this L1 signal is also observed in irradiation-produced bands in the near IR. We therefore defer discussion of its EPR properties until the next section. Seen also in the HVPE sample is a relatively strong zero-phonon line (ZPL) at 0.93 eV with associated phonon structure. This luminescence has previously been reported in GaN and attributed to the V^{3+} impurity.⁹ Observed weakly also with varying intensity in most of the samples is a PL system with ZPL at 1.30 eV which has been identified with Fe^{3+} .⁹

B. After electron irradiation

The visible PL signals are strongly quenched by the electron irradiation in samples A, B, and C. However, the 2.2 eV band, and its associated PLODEPR signals, is still observable, though weaker, in the molecular-beam-epitaxy (MBE)-grown samples D.

In all samples, two new overlapping PL bands are produced by the irradiation in the near-IR (Fig. 2). One, the broad band centered at ~ 0.95 eV in Fig. 2(b), can be produced by all of our excitation energies down to and including 1.52 eV. The other, with the sharp ZPL at 0.88 eV and associated phonon-assisted structure shown in Fig. 2(a), can be excited only with energies down to 2.4 eV, being lost for our next lowest available 1.61 eV laser line. This difference in excitation properties has allowed their separation in Fig. 2. In most of our studies to follow, however, we used near band-gap excitation, where they are simultaneously present. The polarization of the broad 0.95 eV luminescence appears isotropic, but the 0.88 eV system displays preferential polarization along the *c* axis, $\sim 2:1$. Little evidence of saturation for either PL band was observed for above (3.53 eV) or below band-gap (3.41 eV) excitation over the range of excitation powers used in our experiments (≤ 20 mW).

(Very recently, Buyanova *et al.*¹⁰ have reported a somewhat more detailed study of the PL changes in GaN upon electron irradiation. In addition to confirming our previously reported quenching of the visible and near-UV bands and the emergence of the two dominant IR bands described above, they have observed other bands which emerge and disappear at intermediate dosages, depending upon the conductivity

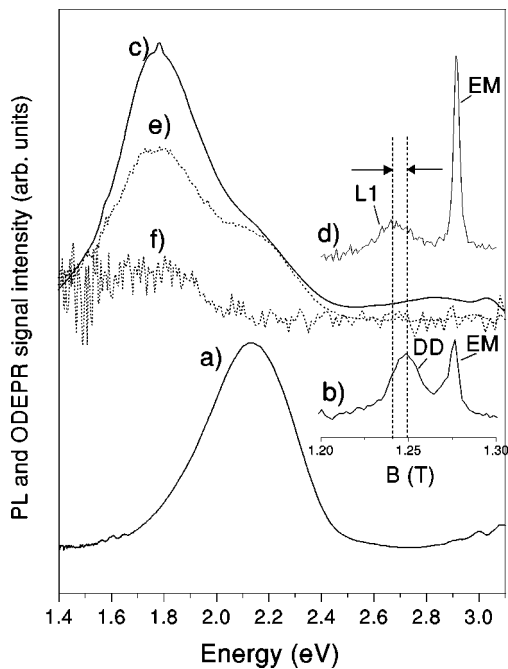


FIG. 1. (a) Visible PL in the MOVPE (A,B) and MBE (D) samples, with (b) corresponding PLODEPR signals. (c) Visible PL in the HVPE sample (C), with (d) its corresponding PLODEPR. Spectral dependence in the HVPE sample for (e) the EM donor, and (f) L1.

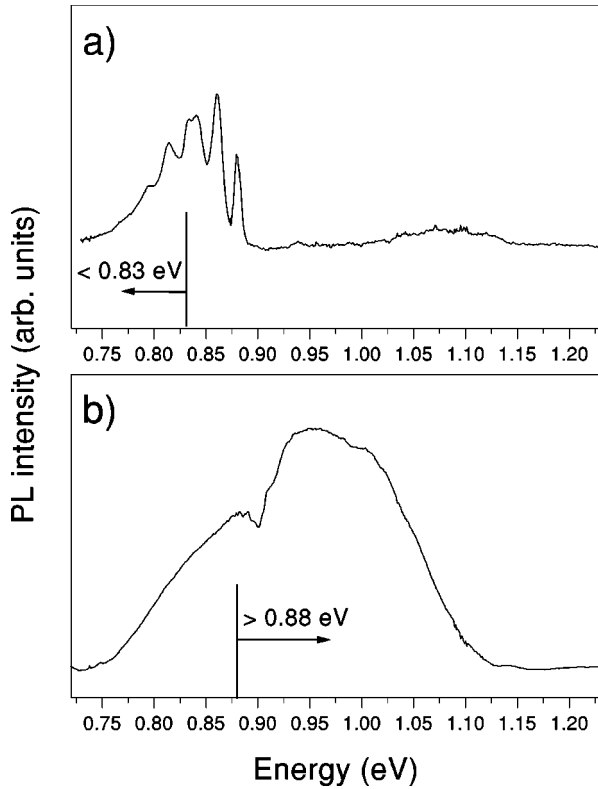


FIG. 2. PL in the near-IR produced by electron irradiation in all of the samples. Indicated are the ranges of the two filters used to separate the PLODEPR spectra from (a) the structured PL with ZPL at 0.88 eV and (b) the broad PL band centered at ~ 0.95 eV.

type of the material. We here concentrate only on ODEPR studies of the two IR bands which dominate after dosages $\sim 10^{18}$ e/cm 2 .)

Four new ODEPR spectra are detected in these IR bands, which we here label L1–4. (In our present study, we find that the signal we previously labeled LE4,^{2,3} is actually part of what we had labeled LE2. We therefore here relabel the spectra, dropping the E to avoid later confusion. LE1 becomes L1, LE2 and LE4 become L2, and LE3 becomes L3, as indicated in Table II. L4 is an additional spectrum.) Their spectral dependences, shown in Fig. 3, reveal that L1 and

TABLE II. Spin-Hamiltonian parameters for the L1–L4 ODEPR defects. The notation in parenthesis after each defect label denotes its previous label.^{2,3} The z axis is the crystal c axis. The number in parentheses after each entry denotes the uncertainty in its last digit.

	L1 (LE1)	L2 (LE2,4)	L3 (LE3)	L4
S	1/2	1	1/2	1/2
g_z	2.008(1)	2.002(2)	1.998(1)	1.998(1)
g_x	2.004(1)	2.002(2)	1.998(1)	1.998(1)
g_y	2.004(1)	1.997(3)	1.998(1)	1.998(1)
D_z (GHz)		$\pm 0.54(1)$		
D_x (GHz)		$\pm 0.33(3)$		
D_y (GHz)		$\mp 0.87(3)$		
$^{69}A_z$ (GHz)			1.90(5)	3.45(5)
$^{69}A_{\perp}$ (GHz)			1.60(5)	3.10(5)

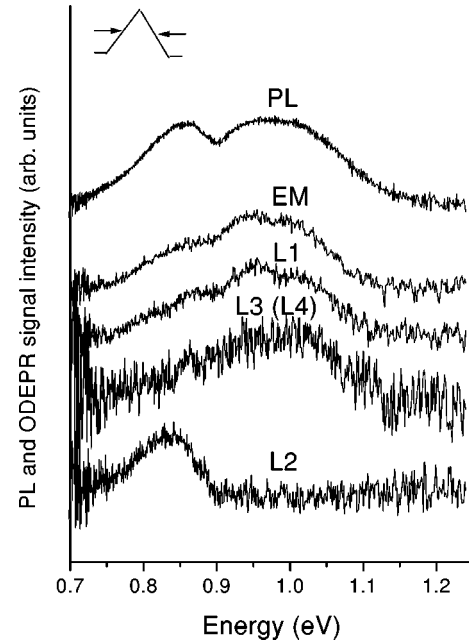


FIG. 3. Spectral dependences of the various PLODEPR signals, compared to the luminescence, under low spectral resolution.

L3(L4) originate from the broad band. (The L4 resonance is too weak for direct spectral dependence studies through the monochromator, but its intensity relative to L3 vs the spectral filters indicated below appears constant suggesting similar dependence for it.) In one of the samples (D, MBE-grown), the shallow donor resonance (EM) is also observed in the broad band, and its spectral dependence is also shown. The spectral dependence of L2 reveals, however, that it originates solely from the structured 0.88 eV system. The runs for Fig. 3, performed at the indicated low resolution to obtain adequate signal to noise, could not reveal the structure of the 0.88 eV band. The results of a slower, signal-averaged scan at higher resolution for L2 is shown in Fig. 4, which confirms the presence of the structure as well.

For adequate signal to noise in the PLODEPR studies, the two overlapping bands were partially separated using either a

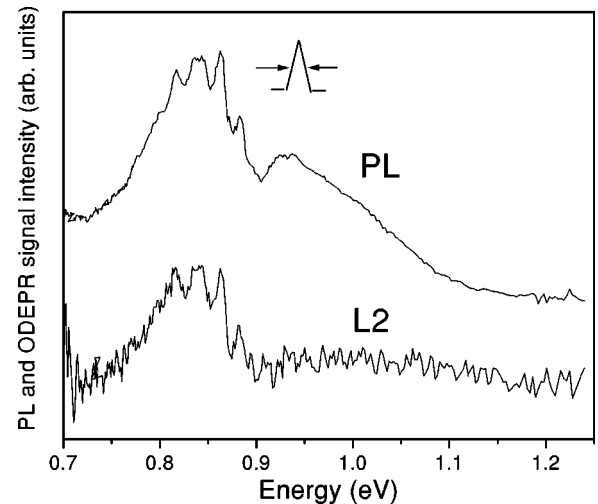


FIG. 4. Spectral dependence of L2 compared to the PL, under higher resolution.

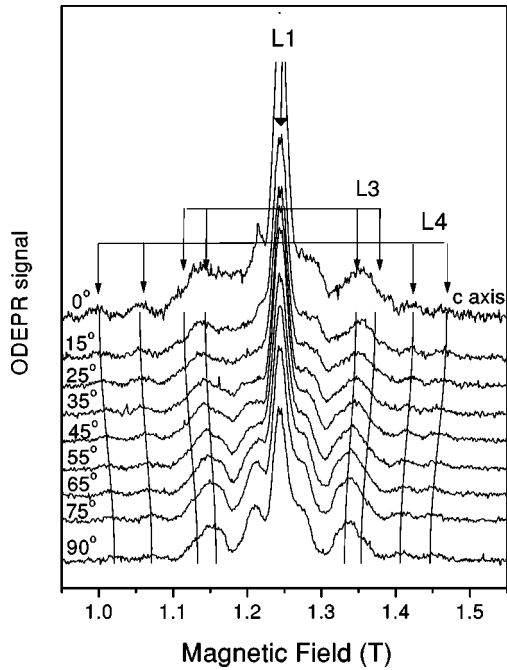


FIG. 5. Angular dependence of L1, L3, and L4 observed in the broad 0.95 eV band.

1.5 μ long pass (<0.8 eV) or 1.4 μ short pass (>0.88 eV) interference filter, the otherwise full IR luminescence being focused on the detector. These selection limits are indicated in Fig. 2. The resulting spectra for the two bands, and their angular dependences, are shown in Figs. 5 and 6. In the following, the spectra for each of the defects has been analyzed using the spin Hamiltonian, applicable for electronic spin $S \geq 1/2$,

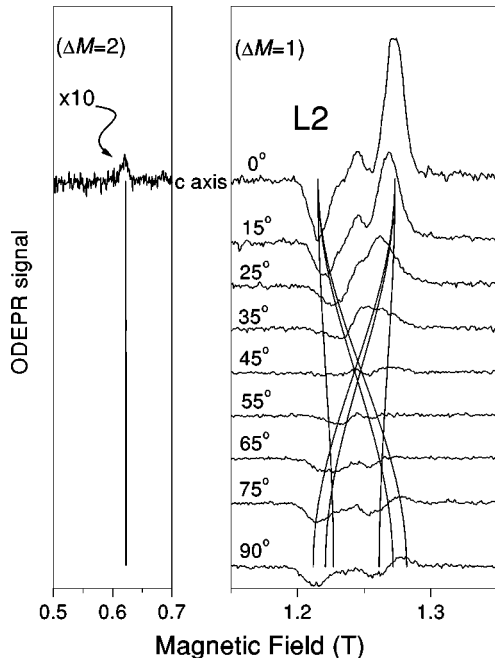


FIG. 6. Angular dependence of the $\Delta M=1$ L2 spectrum observed in the 0.88 eV PL system, showing also the $\Delta M=2$ transition at half the field. The solid lines give the theoretical fit using the parameters of Table II.

$$\mathcal{H} = \mu_B \mathbf{S} \cdot \mathbf{g} \cdot \mathbf{B} + \mathbf{S} \cdot \mathbf{D} \cdot \mathbf{S} + \mathbf{S} \cdot \mathbf{A} \cdot \mathbf{I}, \quad (1)$$

where μ_B is the Bohr magneton, \mathbf{B} the external magnetic field, \mathbf{D} the fine-structure tensor, applicable if $S > 1/2$, and, if resolved, \mathbf{A} is the hyperfine tensor coupling to a nuclear spin \mathbf{I} . The results for each of the spectra are given in Table II.

1. L1

L1, shown in Fig. 5, is a single, structureless, slightly anisotropic $S=1/2$ signal present in all of the irradiated samples throughout the broad PL band. It appears to be the same signal (identical g values) as the one also present in the red band of the HVPE-grown sample A, before irradiation. It is seen only for UV excitation (3.53 and 3.41 eV), being absent for excitation energies of 2.73 eV and below, even though the luminescence band is present for excitation energies down to and including 1.52 eV. From this, we conclude that L1 arises from a defect which is involved in a spin-dependent feeding process for the luminescence, but this process cannot be *the* luminescence process itself.

2. L2

L2, shown in Fig. 6, is an $S=1$ center observed in all of the irradiated samples, and is associated only with the sharp structured 0.88 eV band. (In the actual recorded spectrum, a small contribution of L1, L3, and L4 also exists due to the overlap of the broad 0.95 eV band into the <0.83 eV filter region used for the study, see Fig. 2. In Fig. 6, it has been subtracted.) As seen in the figure for $\mathbf{B} \parallel c$ axis, the high-field line is positive, the low-field line negative, and as they cross in their angular dependence they reverse sign. This can be characteristic of an $S=1$ system for which the spin-lattice relaxation time is shorter than the radiative lifetime, allowing Boltzmann equilibrium to occur between the spin- M states. (As mentioned above, we mistakenly analyzed the spectrum in our earlier preliminary reports^{2,3} as arising from two separate $S=1/2$ spectra, labeling the positive signal for $\mathbf{B} \parallel c$ axis LE2, and the negative lower field transition LE4.) Combined with angular studies in the plane perpendicular to the c axis, the spin-Hamiltonian parameters given in Table II are deduced. (In the analysis, an adequate fit to the data was obtained by taking the principal z axis along the [0001] wurtzite crystal c axis, as given in the table. By symmetry, the x and y axes therefore lie one along $[1\bar{1}00]$, the other along $[11\bar{2}0]$, but without detailed crystal structure determination for the films, it is not known which.) The solid lines in the figure show the predicted transitions using these parameters. Consistent also with the $S=1$ identification, the weak $\Delta M = \pm 2$ transition at half the $\Delta M = \pm 1$ magnetic field is also observed, as shown in the figure.

In this case, the L2 signal is seen over the full range of excitation of the 0.88 eV luminescence (down to 2.41 eV, but not 1.61 eV). This, plus its unique identification with the structured 0.88 eV system, strongly suggests that the defect giving rise to the L2 signal is directly involved with the defect producing the luminescence. However, the ODEPR signal appears to saturate somewhat more strongly than the luminescence vs excitation power [40% reduction in the ratio of the ODEPR signal to the luminescence intensity at 20 mW for above band-gap (3.53 eV) excitation]. This suggests that

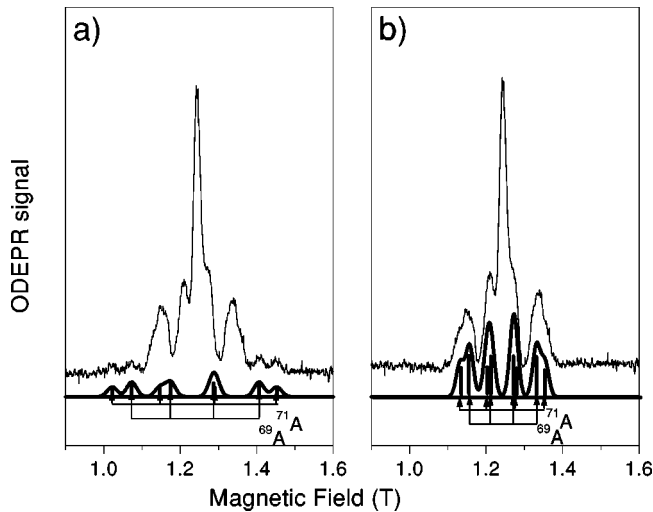


FIG. 7. (a) Match of L4 to the $\mathbf{B} \perp c$ spectrum of Fig. 5, and (b) of L3 after subtraction of the L4 spectrum in (a), using the spin Hamiltonian parameters in Table II.

although it is directly related to the defect producing the luminescence, it may not simply result from an excited $S = 1$ luminescing state of the defect, for which the ODEPR should scale directly with the luminescence. (Consistent with this conclusion, we have also observed the 0.88 eV luminescence in a partially annealed hydrogen-implanted sample but, in that case, no L2 ODEPR signals were observed.¹¹)

3. L3 and L4

L3 and L4 appear in Fig. 5 as the weaker satellites around the strong L1 signal, as shown. (As mentioned in the previous section, the L4 designation is here being reassigned to the weaker further split-out satellites, which were missed in the previous studies.^{2,3}) They both arise from the broad luminescence band only, as shown in Fig. 3. Like the broad luminescence band, they show no evidence of saturation, but their intensities relative to the luminescence drop to zero for excitation at 2.73 eV and below. From this, we can conclude again that, like L1, they are involved in a spin-dependent excitation process for the luminescence but, in each case, the process itself does not uniquely produce the luminescence.

These signals have been seen, but with slightly varying relative intensities, in the irradiated metal-organic vapor phase epitaxy (MOVPE) grown samples A and B, and in the HVPE-grown sample C, but not in the MBE-grown samples (D). In the MBE samples, the broad luminescence is present, but the ODEPR signals observed in them are L1 and, in place of L3 and L4, the shallow donor resonance (EM) usually seen in the 2.2 eV luminescence.

As shown in Fig. 7, the structure of each spectrum can be accurately reproduced as an $S = 1/2$ center with strong hyperfine interaction from a single Ga nucleus (60% ^{69}Ga , 40% ^{71}Ga , both $I = 3/2$). In Fig. 7(a), we show, for \mathbf{B} perpendicular to the c axis, the simulation of the L4 spectrum with the spin-Hamiltonian parameters given in Table II. In Fig. 7(b), after subtracting the simulated L4 spectrum in Fig. 7(a), we show the simulation for L3 with its parameters in Table II. The fit in each case is excellent, as it is for the other orientations of \mathbf{B} .

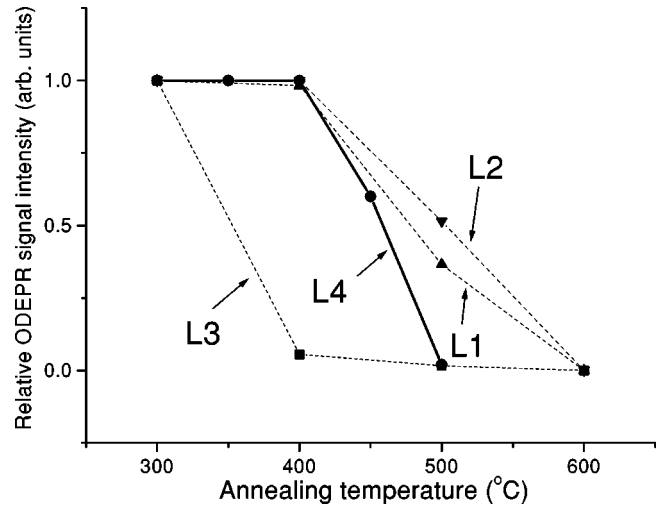


FIG. 8. PLODEPR spectra intensities vs 30 min isochronal anneal. The dashed curves are for one of the MOVPE samples A,² the solid curve for MOVPE sample B.

4. Stability of the defects

In Fig. 8, we show the stability of the defects giving rise to the ODEPR spectra vs an isochronal (30 min) annealing sequence. To the previously published 100 °C interval results³ for L1, L2, and L3 in sample A, we have added new results on a sample from batch B to determine the relative stability of L4, which was missed in the earlier study. In this study, the sample was first annealed for 150 min at 300 °C, which served to remove L3. The subsequent isochronal (30 min) annealing stages were performed at 50 °C intervals, as shown. As reported in the earlier work,³ here also the annealing of the corresponding luminescence bands was observed to correlate approximately with that of the ODEPR spectra.

Not shown in the figure, and noted in our earlier study,³ is the disappearance of an additional signal superposed upon L1 that occurs in the same temperature range that L3 does. As illustrated in Fig. 2 of that paper, its intensity variation vs crystal orientation is significantly different from L1, ruling out its identification with L1, and we discussed the possibility that it might also be part of L3. Our present accurate match of the L3 spectrum shown in Fig. 7 suggests that it is not. Presumably it is related to an additional spectrum which we will not attempt to characterize here. Also not indicated is the weak detection of the EM donor signal in the broad 0.95 eV band after L3 disappears. We cannot completely rule out its presence before the annealing, but it appears to emerge at that point in the anneal.

5. Effects of the GaN/sapphire interface

Excitation of the irradiated samples from the sapphire or GaN side, with either penetrating (3.41 eV, below GaN band gap) or nonpenetrating (3.53 or 3.82 eV, above GaN band gap) excitation, reveals no significant difference between the luminescence intensity or the relative strengths of the individual ODEPR spectra. We can therefore conclude that the defects producing the luminescence and the ODEPR are distributed through the bulk of the GaN layers, and not interface specific. (The equivalence for above GaN band-gap excitation also further confirms that neither the luminescence nor

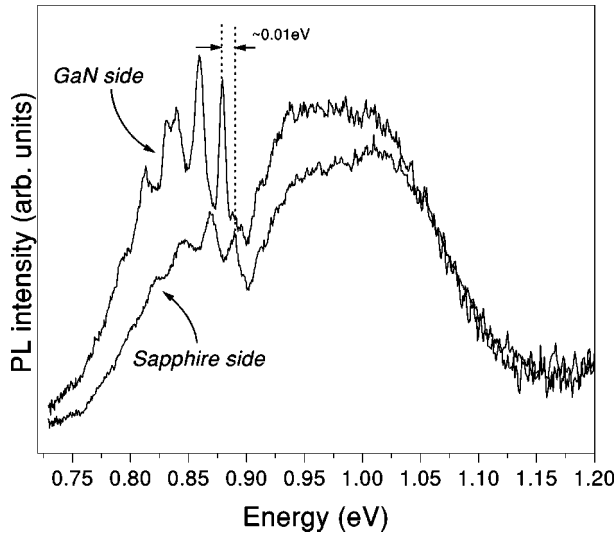


FIG. 9. Difference in the PL spectrum for the HVPE sample for above GaN band-gap excitation from the GaN vs the substrate side.

the ODEPR spectra originate from the sapphire substrate, which is, of course also being electron irradiated.)

However, the sharp 0.88 eV luminescence reveals significant broadening and spectral shifts from sample to sample and vs the direction of excitation that clearly reflect the strain near the interface. This is illustrated in Fig. 9, for above band-gap excitation of the two sides of the thick film (61.3 μm) HVPE sample C. Exciting the GaN side produces the sharp ZPL and phonon-assisted structure expected from a high quality sample with low internal strains. Presumably the thick growth has allowed the material to recover from the interface strain produced in the layer growth by the GaN/sapphire lattice mismatch and differential thermal expansion coefficients. Excitation from the sapphire side, on the other hand, reveals a shift to higher energy of the ZPL by ~ 0.01 eV, and considerable broadening. For the much thinner MOVPE film samples A and B, similar high-energy shifts and broadening are observed, but with little difference between the side of excitation. For the MBE samples (D), a slight shift to lower energies is apparent with only moderate broadening. The observation of similar shifts for the 0.88 eV system have also been reported recently by Buyanova *et al.*¹²

III. DISCUSSION

A. L2 and the 0.88 eV band

The unique connection between L2 and the 0.88 eV structured luminescence band strongly suggests that the ODEPR signal is directly associated with the defect responsible for the luminescence. However, the lack of a constant ratio of L2 signal to luminescence intensity argues that the $S=1$ state detected in L2 is not the emitting excited state giving rise to an $S=1 \rightarrow 0$ luminescence, as is often the case in ODEPR. One possibility is that the emission is actually an allowed transition from an $S=0$ excited state of the defect, for which a nonradiative M -dependent transfer from an energetically close $S=1$ state of the defect is involved. Such a case has been observed for the carbon-carbon pair in silicon, for example.¹³ In that case, alternative excitation paths were evident, as well.

The $S=1$ character of the defect finds further confirmation in some recent results reported by Buyanova *et al.*¹² Although they did not report ODEPR studies, they reported evidence of an energy-level crossing for the emitting defect from enhanced luminescence broadly centered at $B \sim 150\text{--}300$ G, with $\mathbf{B} \parallel c$ axis. Our parameters in Table II predict a level crossing at 200 G, in excellent agreement with their observation. (Actually, they interpreted apparent inflections in their broad derivative signal to result from two crossings, one at ~ 150 G, the other at ~ 300 G. Perhaps their orientation was slightly off the c axis. All of the equivalent orientations of a low-symmetry defect in a wurtzite crystal must superpose for $\mathbf{B} \parallel c$ axis, so actually only one level crossing should occur.)

Without additional hyperfine interactions, the L2 signal unfortunately tells us nothing concerning the chemical or atomic lattice construction of the defect responsible. The strain-related shifts of the 0.88 eV luminescence, however, may reveal something about the electronic structure of the defect. It was pointed out by Buyanova *et al.*¹² that the shifts they observed in the 0.88 eV system correlated with the shifts in the band gap, as monitored by the A, B, C exciton positions observed in the reflectance spectra of the same samples. We find also a 1:1 correspondence between the 0.88-eV ZPL shifts and those observed before irradiation for the bound exciton luminescence line at 3.47 eV in each of the corresponding samples. From this, Buyanova *et al.* suggested that the excited state was a shallow effective-mass-like state close to the conduction band. Consistent with this, they cited thermal quenching studies of the luminescence indicating an activation energy of ~ 30 meV. Taking this value for the excited-state level position below the conduction band, and the ZPL energy of 0.88 eV, they estimated the level position of the defect ground state to be at $E_C - 0.910$ eV. These arguments appear reasonable, but it remains to be seen whether this estimate is consistent with the excitation energy dependence (> 1.61 eV, see Sec. II B 2).

These authors have made the further interesting very recent observation¹⁴ that the phonon structure of the 0.88 eV PL bears a striking similarity to that of the much studied 0.841 eV PL system in GaP. The band in GaP has been attributed to a transition between a shallow $1S(E)$ effective mass state to a deep ground $1S(A_1)$ state of the neutral isolated substitutional oxygen donor.¹⁵ Chen *et al.*¹⁴ suggest therefore that the band is oxygen-related, and, in particular, that it may also be due to the isolated substitutional oxygen donor in GaN. This is clearly consistent with their earlier conclusion that the excited state is shallow EM-like.¹² However, it is surprising that the energy difference between a shallow $1S(E)$ EM state and the deep neutral ground state of a donor would be so insensitive to the band-gap difference of the host (2.26 eV for GaP, 3.51 eV for GaN). This interesting suggestion will therefore require further testing. One obvious test, at least for the incorporation of oxygen, is the effect of oxygen isotope substitution on the ZPL and its phonon structure, as has been established for the 0.841 eV band in GaP.^{15,16}

B. L3 and L4

We can compare estimates of the ^{69}Ga free neutral atom hyperfine interactions for a $4s$ ($a = 7430.4$ MHz) and

$4p$ ($b = 148.2$ MHz) orbital¹⁷ to the observed values of $|A_{\parallel}| = |a + 2b|$ and $|A_{\perp}| = |a - b|$. This leads, for the required fractional components of the wave function on the Ga atom, to $\sim 62\%$ $4p$ and $\sim 23\%$ $4s$ for L3, and $\sim 72\%$ $4p$ and $\sim 43\%$ $4s$ for L4. The wave function in each case is therefore highly localized on a single Ga atom in a $4s$ - $4p$ orbital pointing along the c axis of the crystal.

This is exciting, because these represent ODEPR spectra in GaN with resolved and *identified* hyperfine structure. In addition, in involving a host atom in a configuration produced by the irradiation, they are clearly related to an intrinsic defect in the material. The logical first choice is a Ga interstitial. The fact that there are two similar defects, with different thermal stabilities suggests that it is paired off with some other defect, the result, perhaps, of migration of the interstitial. The failure to see it in the presumably purer MBE material could be interpreted to further support the idea of trapping by trace impurities in the material. Also, the magnitude of the isotropic hyperfine component is similar to that observed in ODEPR spectra of as-grown GaP (2.1 GHz),¹⁸ and $\text{Al}_x\text{Ga}_{1-x}\text{As}$ (1.5 GHz),¹⁹ which were interpreted (correctly or incorrectly) as Ga interstitial related.

However, it should be noted that we cannot completely rule out a highly localized (deep) state of a nitrogen vacancy-related defect. In that case, the unpaired electron could be highly localized on the single c axis Ga near neighbor. This would seem unlikely, the nitrogen vacancy having generally been predicted to be a shallow donor²⁰⁻²² (although not experimentally confirmed). Still, if paired off with another defect, we cannot rule it out.

IV. SUMMARY

Electron irradiation of GaN causes a reduction in the visible and near-UV luminescence bands, while producing two interesting bands in the near-IR. One has a sharp ZPL at 0.88 eV, with well resolved phonon-assisted structure. A well resolved, low-symmetry, $S = 1$ ODEPR spectrum, labeled L2, is detected in the luminescence and identified to be uniquely involved in the defect. It does not appear to be the excited luminescence state of an $S = 1 \rightarrow 0$ optical transition itself, however. Recent studies of the luminescence and its phonon structure by other workers¹⁴ have suggested that oxygen may

be involved, and that the excited state is shallow effective-mass-like.

The other is a broad band centered at ~ 0.95 eV, which reveals three $S = 1/2$ ODEPR signals, L1, L3, L4, plus, in an MBE sample, the EM shallow donor signal, as well. From the lack of 1:1 correspondence between the individual ODEPR intensities and the strength of the luminescence band, we have concluded that for none of the related defects can the spin-dependent process which reveals its spectrum be the actual radiation process. We cannot rule out, however, that at least one of them could be directly related to the luminescing center. For example, spin-dependent charge transfer to an excited state of a defect which then subsequently radiates remains a possibility. Such a case has been cited in ZnS where electron transfer to Fe^{3+} (seen in the ODEPR) produces an excited state of Fe^{2+} which subsequently radiates to its ground state.²³ For such a system, alternative excitation paths can also exist, destroying 1:1 correspondence between ODEPR and luminescence.

L3 and L4 are suggested to be intrinsic-defect related, displaying well resolved hyperfine interactions with a single Ga atom. Analysis reveals the wave function of the unpaired electron to be highly localized for each in a $4s$ - $4p$ orbital on the Ga atom. A model tentatively proposed for the defects is a Ga interstitial trapped by impurities or other defects originally present in the samples.

ACKNOWLEDGMENTS

We acknowledge helpful discussions with M. J. Stavola. We acknowledge also the important roles of A. Doernen, K. Thonke, D. Look, and B. Molnar who facilitated the collaboration between the Lehigh group and the co-authors at Stuttgart, Ulm, MIT/Lincoln Lab, and NRL, respectively, who grew the crystals. The crystal growth program at MIT/Lincoln Lab was sponsored by the U.S. Air Force under Contract No. F19628-95-C-0002 and the opinions, interpretations, conclusions, and recommendations are those of the authors and are not necessarily endorsed by the U.S. Air Force. The research was supported jointly by the National Science Foundation, Grant Nos. DMR-92-04114 and DMR-97-04386, and the Office of Naval Research, Electronics Division, Grant No. N00014-94-10117.

*Present address: Institute of Physics, Polish Academy of Sciences, Warsaw, Poland.

¹For a recent review, see H. Morkoç, *Mater. Sci. Forum* **239-241**, 119 (1997).

²M. Linde, S. J. Uffring, G. D. Watkins, V. Härle, and F. Scholz, *Phys. Rev. B* **55**, R10 177 (1997).

³G. D. Watkins, M. Linde, P. W. Mason, H. Przybylinska, C. Bozdog, S. J. Uffring, V. Härle, F. Scholz, W. J. Choyke, and G. A. Slack, *Mater. Sci. Forum* **258-263**, 1087 (1997).

⁴M. H. Nazaré, P. W. Mason, G. D. Watkins, and H. Kanda, *Phys. Rev. B* **51**, 16 741 (1995).

⁵E. R. Glaser, T. A. Kennedy, K. Doverspike, L. B. Rowland, D. K. Gaskill, J. A. Freitas, Jr., M. Asaaf-Khan, D. T. Olson, J. N. Kuznia, and W. K. Wickenden, *Phys. Rev. B* **51**, 13 326 (1995).

⁶U. Kaufmann, M. Kunzer, C. Merz, I. Akasaki, and H. Amano,

in *Gallium Nitride and Related Materials*, edited by F. A. Ponce, R. D. Dupuis, S. Nakamura, and J. A. Edmond, MRS Symposia Proceedings No. 395 (Materials Research Society, Pittsburgh, 1996), p. 633.

⁷D. M. Hoffmann, D. Kovalev, G. Steude, D. Volm, B. K. Meyer, C. Xavier, T. Monteiro, E. Pereira, E. N. Mokov, H. Amano, and A. Akasaki, in Ref. 6, p. 619.

⁸W. Götz, L. T. Romano, B. S. Krusor, N. M. Johnson, and R. J. Molnar, *Appl. Phys. Lett.* **69**, 242 (1996).

⁹J. Baur, U. Kaufmann, M. Kunzer, J. Schneider, H. Amano, I. Akasaki, T. Detchprohm, and K. Hiramatsu, *Mater. Sci. Forum* **196-201**, 55 (1995).

¹⁰I. A. Buyanova, M. Wagner, W. M. Chen, B. Monemar, J. L. Lindström, H. Amano, and I. Akasaki, *Appl. Phys. Lett.* **73**, 2968 (1998).

¹¹M. G. Weinstein, M. Stavola, C. Y. Song, C. Bozdog, H. Przy-

- bylinska, G. D. Watkins, S. J. Pearton, and R. G. Wilson, MRS Internet J. Nitride Semicond. Res. **4S1**, G5.9 (1999).
- ¹²I. A. Buyanova, M. Wagner, W. M. Chen, B. Monemar, J. L. Lindström, H. Amano, and I. Akasaki, MRS Internet J. Nitride Semicond. Res. **3**, 18 (1998).
- ¹³K. M. Lee, K. P. O'Donnell, J. Weber, B. C. Cavenett, and G. D. Watkins, Phys. Rev. Lett. **48**, 37 (1982).
- ¹⁴W. M. Chen, I. A. Buyanova, M. Wagner, B. Monemar, J. L. Lindström, H. Amano, and I. Akasaki, Phys. Rev. B **58**, R13 351 (1998).
- ¹⁵P. J. Dean, in *Deep Centers in Semiconductors*, edited by S. T. Pantelides (Gordon and Breach, New York, 1986), p. 185.
- ¹⁶P. J. Dean and C. Henry, Phys. Rev. **176**, 928 (1968).
- ¹⁷A. K. Koh and D. J. Miller, At. Data Nucl. Data Tables **33**, 235 (1985).
- ¹⁸K. M. Lee, in *Defects in Electronic Materials*, edited by M. Stavola, S. J. Pearton, and G. Davies, MRS Symposia Proceedings No. 104 (Materials Research Society, Pittsburgh, 1988), p. 449.
- ¹⁹T. A. Kennedy and M. G. Spencer, Phys. Rev. Lett. **57**, 260 (1986).
- ²⁰D. W. Jenkins, J. D. Dow, and M.-H. Tsai, J. Appl. Phys. **72**, 4130 (1992).
- ²¹J. Neugebauer and C. G. Van de Walle, Phys. Rev. B **50**, 8067 (1994).
- ²²P. Boguslawski, E. L. Briggs, and J. Bernholc, Phys. Rev. B **51**, 17 255 (1995).
- ²³K. P. O'Donnell, K. M. Lee, and G. D. Watkins, J. Phys. C **16**, L723 (1983).